Identification of dynamic contact instabilities generated by braking materials

S. Ciprari[1], D. Tonazzi[1], A. Lazzari[1], A. Saulot[2], F. Massi[1]
[1] "Sapienza'' University of Rome, DIMA, Department of Mechanical and Aerospace Engineering, via Eudossiana 18, 00184 Rome, Italy.

[2] University of Lyon, CNRS, INSA Lyon, UMR 5259, LaMCoS - Contacts and Structural Mechanics Laboratory, 20 rue des Sciences, F-69621 Villeurbanne, France.

Abstract
The occurrence of unstable friction-induced vibrations is a major issue for braking manufacturers, as they lead to annoying noise, structure vibrations and brake surface degradation. Understanding the underlying causes of frictional instabilities, arising during the sliding between two bodies, is necessary for developing solutions and countermeasures. For this purpose, in this work, an experimental and numerical investigation of contact instabilities has been performed. Mode coupling and negative friction-velocity slope instabilities have been numerically investigated by both lumped-parameter and finite element models. As well, an experimental campaign has been carried out for recovering the frictional and vibrational response of braking materials under different boundary conditions. The comparison between numerical and experimental results allows validating a new methodology, based on the study of the phase shift between the tangential and normal vibrational responses, in order to distinguish the different types of contact instabilities.

1 Introduction

Friction-induced vibrations (FIV) are an ever-present phenomenon during frictional contacts [1]. Nowadays, the occurrence of undesired contact instabilities arising during braking is one of the major issues faced by the brake industry [2, 3]. According to [1], this phenomenon represents a large warranty cost for brake manufacturers and reaches almost one billion dollars per year in North America. More in general, contact instabilities can occur in any mechanical system with a frictional interface [4, 5] and consequently the understanding of such complex phenomena is relevant for many industrial and research applications such as endoprosthesis squeaking [6, 7] , false brinelling in rolling bearings [8], stick-slip in piezo actuator [9], etc. As a consequence, significant amount of research works aim to investigate and mitigate the occurrence of undesired noise [10, 11] and surface degradation due to such unstable frictional responses. Many works deal, both numerically and experimentally, with friction-induced vibrations [12] and related instabilities [11, 13, 14]. Despite this, in real industrial problems, it is often difficult to distinguish the occurrence of unstable friction-induced vibrations due to different mechanisms, such as mode coupling [14-16] and negative friction-velocity slope [17]. However, understanding the nature of the contact instabilities is important to identify effective countermeasures to prevent their occurrence. Within this framework, this paper aims to investigate the frictional and vibrational response of a braking material, and to analyse its propensity to destabilize the dynamics [18] of the system when subjected to different boundary conditions during frictional contact. The frictional response is investigated as a function of temperature and relative sliding velocity. The resulting vibrational response, under the combination of these parameters, is retrieved, analysed, and then compared with the vibrational phenomena reproduced numerically. This procedure allowed for the identification of the experimentally observed instabilities. More in detail, an approach, based

on the analysis of the phase shift between normal and tangential accelerations, is proposed to discriminate a mode coupling instability from a negative friction-velocity slope instability.

2 Lumped parameters model

Lumped-parameter models are an effective tool for studying friction-induced vibrations and contact instabilities [19-21]. With the aim of investigating and characterizing different types of unstable friction-induced vibrations (i.e., mode coupling and negative friction-velocity slope), a lumped parameter model has been developed and implemented on Simulink. In the following paragraphs, first, a model description is provided and the motion equations are presented. Then, a complex eigenvalue analysis of the model is provided as a function of the friction coefficient. After that, the different types of unstable friction-induced vibrations and their coexistence are simulated by transient simulations and then analysed.

2.1 Model description

The developed lumped-parameter model consists of two masses, one of which in frictional contact with a moving belt, as shown in Figure 1.

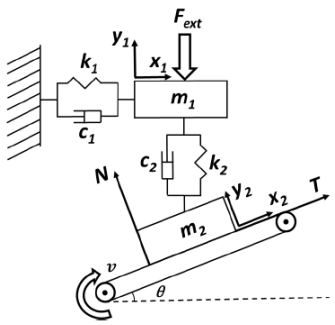

Figure 1: Lumped-parameters model

As shown in Figure 1, the mass m_1 is connected to a frame with an horizontal spring-damper system, while the other is in frictional contact with a moving belt. The two masses are connected by a vertical spring-damper system. On the horizontal direction this connection results rigid and, therefore, a mutual horizontal force F_0 is exchanged at the two ends of the connection. The system is subjected to an external vertical force that pushes the second mass in contact with the belt, which is inclined of an angle θ. The model parameters (Table 1) have been chosen to qualitatively simulate the different contact instabilities (mode coupling and negative slope), as a function of the introduced friction law.

Table 1:Model parameters chosen for the analysis

PARAMETER	m1	m2	k1	k2	c1	c2	V_{belt}	F_{ext}	θ
VALUE	2.12 [kg]	0.18 [kg]	100000 [N/m]	101000 [N/m]	0.1 [Ns/m]	0.1 [Ns/m]	7 → 0 [m/s]	1000 [N]	0.01 rad

The system equations are reported in the following lines. Starting from the mass m_1 the equilibrium can be written as:

$$\begin{gathered} m_1\ddot{x}_1 + c_1\dot{x}_1 + k_1x_1 + F_0 = 0 \\ m_1\ddot{y}_1 + c_2(\dot{y}_1 - \dot{y}_2\cos\theta - \dot{x}_2\sin\theta) + k_2(y_1 - y_2\cos\theta\ - x_2\sin\theta) + F_{ex}\ =\ 0 \end{gathered} \tag{1}$$

And for the mass m_2:

$$\begin{cases} m_2\ddot{x}_2 + c_2(\dot{x}_2 \sin\theta + \dot{y}_2 \cos\theta - \dot{y}_1)\sin\theta + k_2(x_2 \sin\theta + y_2 \cos\theta - y_1)\sin\theta = T + F_0 \cos\theta \\ m_2\ddot{y}_2 + c_2(\dot{x}_2 \sin\theta + \dot{y}_2 \cos\theta - \dot{y}_1)\cos\theta + k_2(x_2 \sin\theta + y_2 \cos\theta\ - y_1)\cos\theta = N - F_0 \sin\theta \end{cases} \quad (2)$$

The DOF of the system, that is initially equal to four, since two directions for each mass have been considered, can be reduced imposing the rigid motion along the horizontal direction of the two masses, expressed by the condition $x_1 = x_2 \cos\theta$. The resulting system, after performing the appropriate substitutions, can be rewritten in a matrix form as follows:

$$\bar{\bar{M}}\underline{\ddot{r}} + \bar{\bar{C}}\underline{\dot{r}} + \bar{\bar{K}}\,\underline{r} = \underline{F} \quad (3)$$

Where:

$$\bar{\bar{M}} = \begin{bmatrix} m_2 + m_1\cos^2\theta + \mu_d m_1 \cos\theta \sin\theta & 0 \\ 0 & m_1 \end{bmatrix}$$

$$\bar{\bar{C}} = \begin{bmatrix} c_2\, sin^2\theta\ +\ c_1\, cos^2\theta\ + \mu_d(c_1 - c_2)\cos\theta \sin\theta & -c_2 \sin\theta + \mu_d c_2 \cos\theta \\ -c_2 \sin\theta & c_2 \end{bmatrix}$$

$$\bar{\bar{K}} = \begin{bmatrix} k_2\, sin^2\theta + k_1\, cos^2\theta + \mu_d(k_1 - k_2)\cos\theta \sin\theta & -k_2 \sin\theta + \mu_d k_2 \cos\theta \\ -k_2 \sin\theta & k_2 \end{bmatrix}$$

$$\underline{r} = \begin{pmatrix} x_2 \\ y_1 \end{pmatrix} \underline{F} = \begin{pmatrix} 0 \\ -F_{ex} \end{pmatrix} \quad (4)$$

The equation of motion described in (4) has been retrieved assuming a sliding contact between the mass m_2 and the sliding belt. However, the model allows considering also other contact conditions such as detachment and sticking conditions. The developed MATLAB code checks first if the conditions for the contact of m_2 with the belt are met. That happens when the normal force $N > 0$ and $y_2 \leq 0$. If these conditions are not both satisfied the system is in a detachment status. In such a case, the equation of motion account for the further degree of freedom along y_2. If the conditions $N > 0$ and $y_2 \leq 0$ are both satisfied the code checks for a sticking or a sliding condition. If the relative velocity between the mass and the belt is zero (with a certain tolerance) and $T \leq \mu_s N$ is satisfied, the contact is in sticking. For transient simulations, the integration time step has been chosen very small ($dt = 10^{-4}s$) with respect to the period of oscillations, to ensure an adequate sampling of the obtained signals and convergence of the solver.

2.2 Modal analysis

As a first step of the analysis, a complex eigenvalue analysis has been carried out as a function of the friction coefficient. The analysis is performed on an equilibrium state in contact sliding condition, using the equations described in (3) (3) and (4). The results of the analysis are shown in Figure 2.

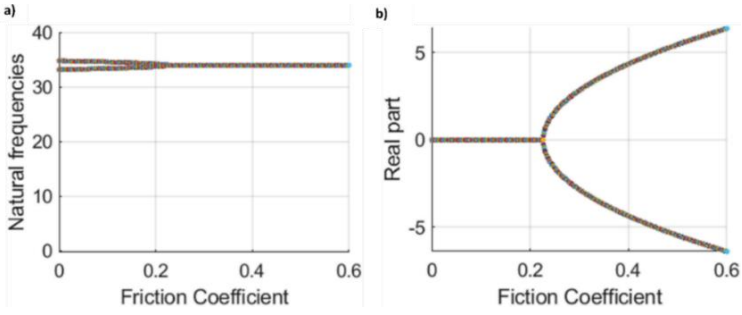

Figure 2 : Natural frequencies of the system (a) and real part of eigenvalues (b), as a function of the friction coefficient

From Figure 2 it can be noted that, for the chosen parameters, the system is incurring in mode coupling at a friction coefficient equal to 0.22, for which the two modes coalesce in a single one, with a frequency around 34 Hz. From the critical value of the friction coefficient (i.e., 0.22), the real part of the eigenvalues shows a

bifurcation. This leads to a positive real part of one of the eigenvalues and, therefore, to self-excited unstable friction-induced vibrations. The mode coupling instability can be induced, for this reason, imposing a friction law characterized by a dynamic friction coefficient higher than the critical value. For lower values, when the friction coefficient stays constant, the system is expected to be stable.

2.3 Transient stability analysis

In the following sections, mode coupling and negative slope instabilities, as well as their superposition, are analysed in detail. Firstly, the friction laws used in the simulations are described. Then, the vibrational response obtained by the simulations are discussed. Lastly, particular attention is given to the phase shift between the tangential and normal vibrational signals close to the contact. The study of different types of instabilities has been performed by the imposition of adequate friction laws. The friction laws used to simulate negative slope instability, mode coupling instability, and the coexistence of these two types of instability, are presented in Figure 3.

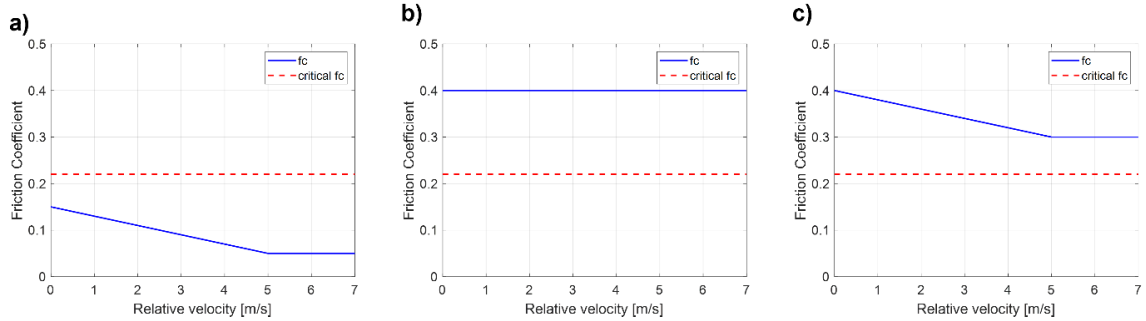

Figure 3: Friction-velocity laws used to simulate negative slope instability (a, $\mu_s = 0.15, \mu_d = 0.05$), mode coupling instability (b, $\mu_s = \mu_d = 0.4$) and the coexistence of the two instabilities (c, $\mu_s = 0.4$, $\mu_d = 0.3$)

Bilinear friction laws have been chosen for the analysis. The friction coefficient remains constant and equal to the dynamic one until the relative velocity is larger than 5m/s. When the relative velocity decreases under this value, the friction coefficient rises linearly to the static friction coefficient. As can be seen from Figure 3a, in order to avoid the superposition with mode coupling instability, the chosen values of the friction coefficients for simulating the negative slope instability are μ_s = 0.15 and μ_d = 0.05, both lower than the critical value of 0.22, which leads to the merging of the modes (see Figure 2). To simulate mode coupling instability, a constant friction law has been imposed (Figure 3b). The chosen value of the friction coefficient ($\mu_s = \mu_d$ = 0.4) is larger than the critical friction coefficient that leads to the merging of the modes. A static friction coefficient equal to the dynamic one allows decoupling the occurrence of the mode coupling from the negative friction velocity slope instability. As visible from Figure 3c, to induce the coexistence of negative slope and mode coupling instability, a bilinear friction law (μ_s = 0.4 and μ_d = 0.3) has been imposed. The chosen values for dynamic and static friction coefficient are both larger than the critical friction coefficient. The results obtained by the simulations performed imposing the described friction laws are reported in the following sections.

2.3.1 Negative slope instability

This type of instability appears when an increasing friction coefficient with a decreasing relative velocity is present. A negative friction-velocity gradient leads to a negative apparent damping and, therefore, to the onset of a dynamic instability. The vibrational response of the system, obtained under the bilinear friction law (μ_s=0.15, μ_d=0.05), is reported in Figure 4.

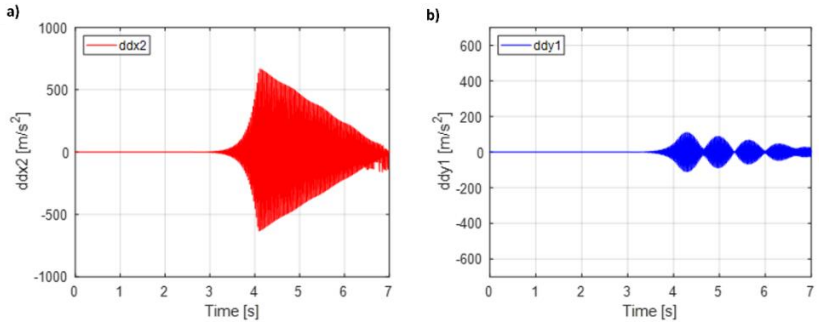

Figure 4: Tangential (ddx2, a) and normal (ddy1, b) accelerations, obtained for variable imposed velocity of the belt (7 → 0 m/s) and bilinear friction law (μ_s=0.15, μ_d=0.05)

As can be seen from Figure 4, until the critical velocity is reached, the system shows a stable vibrational response. When the negative slope part of the friction law is reached, vibration amplitudes start growing exponentially, up to a limit cycle. Once the limit cycle is reached, the vibration amplitude starts decreasing, due to the linear decrease of the imposed velocity to the belt. This results in a decreasing energy injected by the contact. Since the friction coefficient is lower than the critical one, lock-in does not occur. Nevertheless, the two modes are very close in frequency (see Figure 2a) and a beat phenomenon is observed in the vertical acceleration (Figure 4b).

2.3.2 Mode coupling instability

Mode coupling instability has been investigated using the constant friction law described in Figure 3b. Both static and dynamic friction coefficient (μ_s=μ_d=0.4) are higher than the critical value of 0.22 (see Figure 2). Being the friction coefficient higher than the critical friction coefficient (at which the lock-in phenomenon occurs, see Figure 2), the dynamic response of the system results in unstable friction-induced vibrations. The acceleration signals in the x2 and y1 directions, describing the dynamic response of the system, are shown in Figure 5:

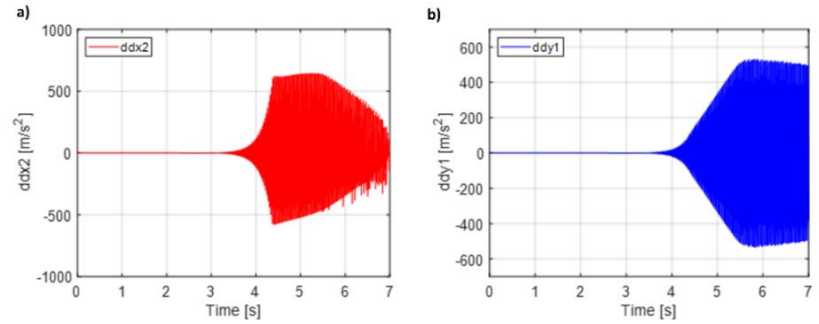

Figure 5: Tangential (ddx2, a) and normal (ddy1, b) accelerations, obtained for variable imposed velocity of the belt (7 → 0 m/s) and constant friction law μ_s=μ_d=0.4

Along the tangential and normal directions, exponentially increasing vibrations can be clearly identified. When the limit cycle is reached, the tangential vibration amplitude decreases. Because the instability here is caused by the unstable eigenvalue, and is not purely related to the variation of friction with the velocity, the decrease of the limit cycle amplitude with the velocity is not linear, but is characterized by a almost stable zone, followed by the decreasing. This is in agreement with works on brake squeal [22, 23], showing a saturation of the amplitude of the limit cycles with the sliding velocity. Comparing Figure 4a and Figure 5a, under the system parameters described in Table 1, the amplitude of the tangential accelerations, obtained by either the negative friction-velocity slope instability or the mode coupling instability, show similar

values. The coexistence of the two instabilities can be, therefore, investigated avoiding that the effect of an instability is predominant on the other. The analysis on the coexistence of the two instabilities is discussed in the next paragraph.

2.3.3 Coexistence of mode coupling and negative friction-velocity slope instabilities

The superposition of the two instabilities has been analysed imposing the friction law described in Figure 3c. This type of friction law ($\mu_s = 0.4$, $\mu_d = 0.3$) combines both negative friction-velocity slope and friction values larger than the critical friction coefficient. The obtained vibrational response is shown in Figure 6:

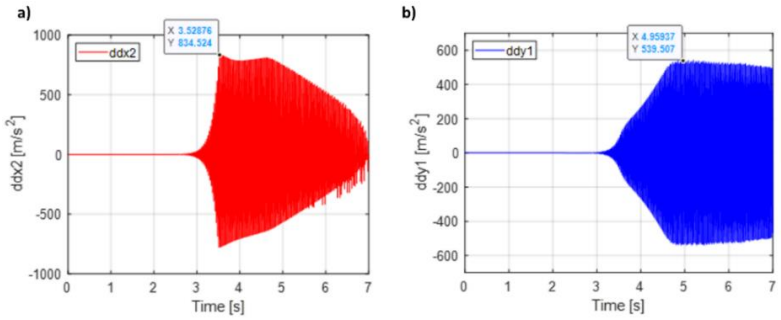

Figure 6: Tangential (ddx2, a) and vertical (ddy1, b) accelerations, obtained for variable imposed velocity of the belt (7 → 0 m/s) and bilinear friction law (μ_s=0.4, μ_d=0.3)

As can be seen comparing Figure 6 with Figure 4 and Figure 5, the maximum values of both the accelerations are larger than the one obtained with a single instability. The superposition of the effects is, therefore, possible under a friction law with values larger than the critical one and a negative slope with respect to the sliding velocity.

2.4 Phase shift analysis

The phase shift between normal and tangential accelerations has been analysed for both mode coupling and negative slope instability. It has been verified before the onset of the detachment, during the exponential increase of vibrations, because non-linearities, such as the detachment, introduce harmonics that modify the signals and make more difficult the direct comparison. A negative slope instability (μ_s= 0.07 μ_d= 0.02) and a mode coupling instability ($\mu_s = \mu_d = 0.8$), both far from the bifurcation point, have been analysed. The acceleration signals and their zoom, taken during the exponential increase, are shown in Figure 7.

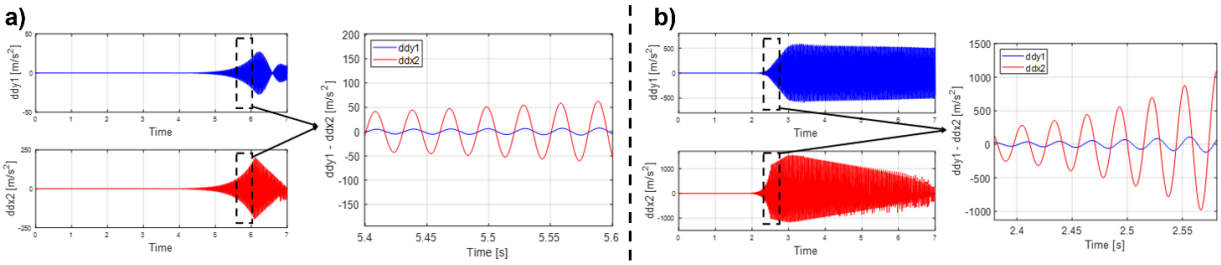

Figure 7: Tangential (ddx2, red) and normal (ddy1, blue) accelerations for negative slope (a, μ_s= 0.07 μ_d= 0.02) and mode coupling (b, $\mu_s = \mu_d = 0.8$). A zoom taken during the exponential increase of the two signals is, also, reported. Obtained for variable belt velocity (7 → 0 m/s).

As can be seen from Figure 7a, the normal and tangential accelerations, resulting from a negative slope instability, are in phase. As concerns mode coupling, as can be seen from Figure 7b, the two accelerations are almost in quadrature. In fact, for an undamped system, the phase shift between normal and tangential accelerations is expected to be almost equal to 90° [2]. In mode coupling instability, this phase shift allows the energy flux between the normal and tangential direction [19, 24]. From the analysis carried out so far, it can be noticed that the phase shift can be used as a method to distinguish the two different instabilities, i.e., mode coupling and negative friction-velocity slope instability. In fact, when a mode coupling instability occurs, the normal and tangential accelerations are in quadrature. Instead, when a negative slope instability occurs, the normal and tangential accelerations are in phase.

3 Experimental analysis

In order to experimentally characterize the frictional and vibrational response of braking materials, which can present both mode-coupling and negative-slope instabilities, tests have been carried out on a dedicated test bench, named TriboAir. First, in the following section, a description of the test bench and of the samples is provided. Then, the measurement campaign protocol and the test conditions are presented. Finally, the analysis of the different tests and the identification of the observed instabilities is carried out.

3.1 Experimental set-up

The used experimental set-up (Figure 8) allows studying the effect of the several parameters, such as temperature, velocity and contact pressure, on the frictional and vibrational response. The material propensity to destabilize the dynamics of the frictional system can be investigated under well-controlled boundary conditions. This test bench also ensures that parasitic vibrations, coming from external sources are avoided.

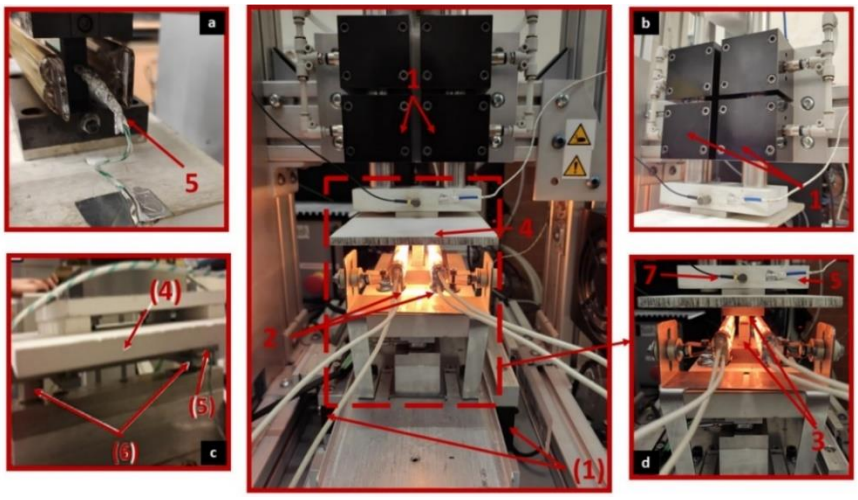

Figure 8: Experimental set-up TriboAir: 1. Air Bearings, 2. IR Lamps, 3. Samples, 4. Insulation System, 5. Thermocouples, 6. Force Transducers, 7. Accelerometer

Air bearings (1) allow for the relative motion of the lower moving part of the test bench, with respect to the upper one, which can move along the vertical direction for imposing the load (Figure 8b). Air bearings also prevent the occurrence of parasitic vibrations. The load is imposed trough dead weights and it has been fixed to 17N. The air guide shown in Figure 8b avoids any vertical friction that could alter the imposed load. The imposed motion law, to the lower sample, is ensured by a linear voice coil (BEI KIMCO LA30-75-001A), driven by a servo drive (HARMONICA) and an optical encoder, which allow for the motion feedback

control. In order to characterize the frictional behaviour of the tested material at different temperatures, two IR linear emitters are used (2). They are mounted on the lower part of the test bench and positioned parallel to the two samples (3). Their tungsten filament emits short IR waves and can reach a temperature of 1200 °C. A thermal insulation, consisting of two ceramic plates (4), allows best conveying heat to the contact interface and protecting the transducers. A thermocouple (5, Figure 8a) is positioned inside the lower sample, as close as possible to the contact interface, in a hole positioned 3mm under the contact surface. Its signal is recorded and given to a PID controller, that allows for the sample temperature control. The 3-axial force transducers (6, Figure 8c) KISTLER 9017B records the force in both vertical and tangential directions, allowing to retrieve the friction coefficient, used to characterize the frictional response of the material. An accelerometer (7, Figure 8d) allows for recording the friction-induced vibrations. Measurements of the force and acceleration of the system are recorded using the acquisition system (SIRIUS–DEWESOFT), based on DualCoreADC® technology with dual 24-bit delta-sigma analogue to digital converter (ADC). An anti-aliasing filter on each analogue channel achieves a 160 dB dynamic range in time and frequency domains with 200 kHz sampling rate per channel. Data are post-processed by MATLAB. As concerns the frictional material samples, the lower sample, clamped on the lower moving part, is a parallelepiped with a rectangular contact surface of 50x10mm. The upper fixed sample is a cube with a dimension of 10mm. The possible sliding distance is, therefore, 40mm for each stroke.

3.2 High temperature measurement campaign

The experimental tests aim to characterize the frictional and dynamic response of the frictional material samples under different conditions of temperature and sliding velocity. The obtained signals are analysed and compared with the results obtained from the numerical 3DOFs model, described in 2.1. In the following sections, firstly, the test conditions are described. Secondly, the post-processing carried out on the retrieved signals is presented. Finally, the system frictional and dynamic response is presented.

3.2.1 Test conditions

In order to characterize the material response two types of tests are carried out: constant sliding velocity and variable sliding velocity tests. The motion laws used for each type of test are described in Figure 9.

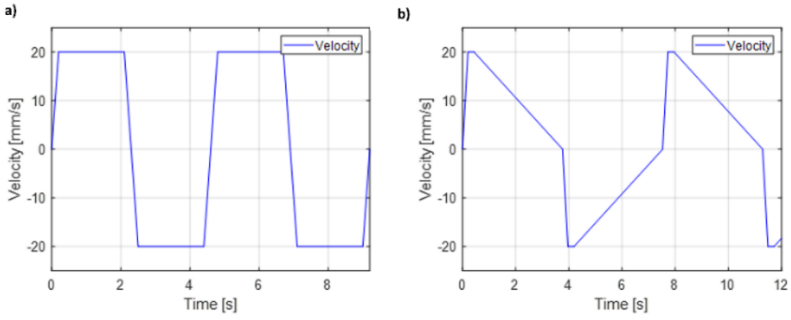

Figure 9: Constant velocity (a) and variable velocity (b) motion laws

A decreasing relative velocity (Figure 9b) allows for the investigation of the tribological and dynamical response of the tested samples during braking. Constant relative velocity tests (Figure 9a), through the comparison with the variable velocity tests, allows decoupling the effect of the sliding velocity on the frictional and vibrational response of the tested materials. For both types of tests, different temperature conditions are imposed. Three different temperatures (HT) have been used for each type of test: 100°C, 300°C and 500°C. Before performing the first test, a running-in of the samples is carried out to ensure a well-established contact between the contacting surfaces.

3.2.2 Signal analysis

To introduce the analysis performed on the experimental retrieved signals, an example of a single sliding stroke, taken at room temperature condition from a variable velocity test, is shown in Figure 10.

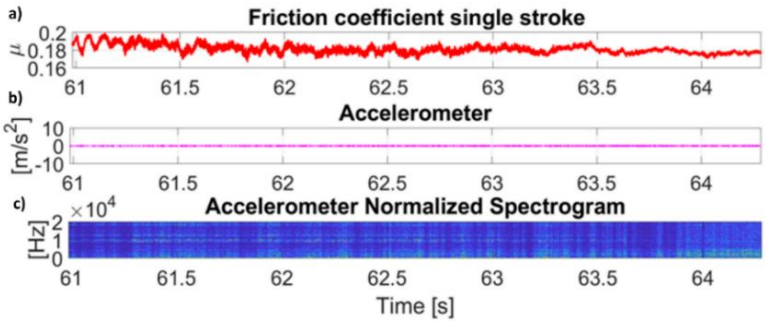

Figure 10: Example of signal analysis on a stable single stroke. Friction coefficient (a), accelerometer signal (b) and accelerometer normalized spectrogram (c) are shown. Obtained from a variable velocity test, at room temperature (RT) condition

As can be seen from Figure 10, the single stroke has been post-processed to retrieve the friction coefficient (Figure 10a), the accelerometer signal (Figure 10b) and the acceleration spectrogram (Figure 10c). The spectrogram has been obtained with a time window of 0.01s and an overlap of 98% between two consecutive time windows. Moreover, the spectrogram has been normalized with respect to the maximum value of each window.

3.2.3 Experimental tests

3.2.3.1 HT 300°C variable velocity

The frictional and vibrational response of a single stroke, taken at 300 °C, under variable velocity motion conditions, is reported in Figure 11.

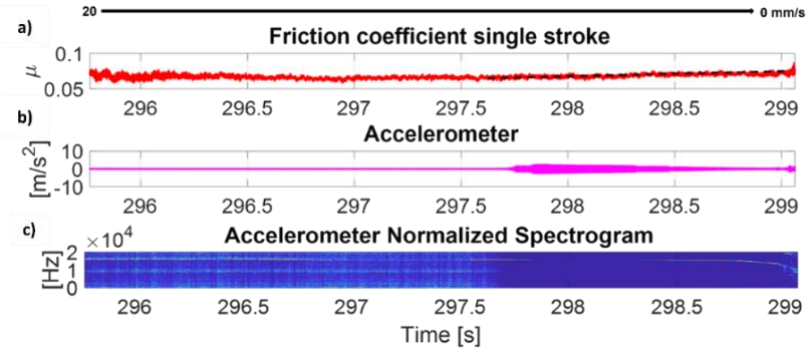

Figure 11: 300°C single stroke: friction coefficient (a), accelerometer signal (b) and accelerometer normalized spectrogram (c). Obtained from HT 300°C variable velocity test

As can be seen from Figure 11a, the friction coefficient shows low values at 300°C. Such low values, as visible in the first part of the stroke, are not sufficient to induce a mode coupling instability. It can be, therefore, assumed that the critical friction coefficient that leads to the merging of the modes is higher than the observed one. Moreover, a slight negative friction-velocity slope is observed at the end of the stroke. In correspondence of this negative friction-velocity slope, unstable vibrations are recognizable from the

accelerometer signal (Figure 11b) and from the accelerometer spectrogram (Figure 11 c). As can be seen from Figure 11b, the amplitude of the unstable vibration reduces during the stroke. This is attributable to a velocity reduction and, therefore, to a lower energy immitted into the system through the frictional contact. This phenomenon has been already observed in variable velocity simulations performed with the Simulink model (Figure 4).

3.2.3.2 HT 500°C constant velocity

A single stroke, taken in correspondence of a temperature of 500°C under constant velocity motion conditions, is analysed in Figure 12.

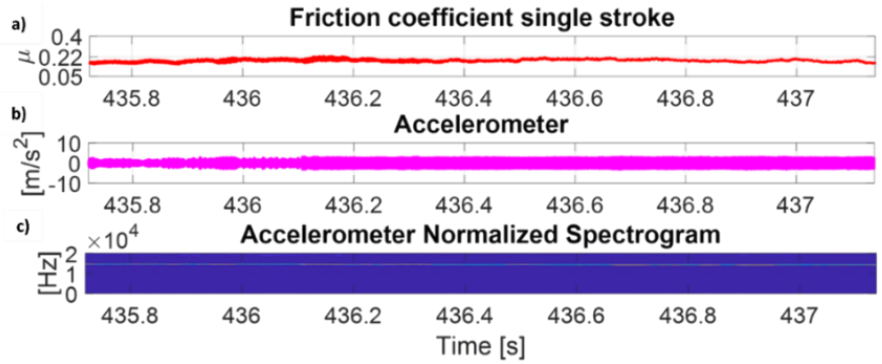

Figure 12: 500°C single stroke: friction coefficient (a), accelerometer signal (b) and accelerometer normalized spectrogram (c). Obtained from HT 500°C constant velocity test

As can be seen from Figure 12a, the dynamic friction coefficient is slightly higher than 0.2. The negative friction velocity-slope observed in Figure 11 is not present. The vibrational response, shown in Figure 12b, shows unstable friction-induced vibrations during the whole stroke. Since it is not present a negative friction-velocity slope, the unstable response can be attributed to the sole mode coupling instability.

3.2.3.3 HT 500°C variable velocity

A single stroke, taken in correspondence of a temperature of 500°C from HT 500°C variable velocity test, is analysed in Figure 13:

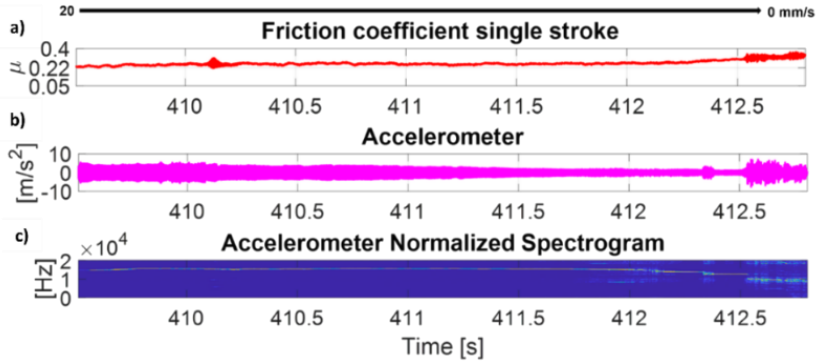

Figure 13: 500°C single stroke: friction coefficient (a), accelerometer signal (b) and accelerometer normalized spectrogram (c). Obtained from HT 500°C variable velocity test

Comparing Figure 13 with Figure 11, two main differences can be observed:

- The values of the dynamic friction coefficient at 300 °C (Figure 11a) are lower than the 500 °C ones (Figure 13a).

- The variation of the friction coefficient that can be observed during the single stroke at 300 °C (Figure 11a) is as well observed at 500 °C (Figure 13a).

The effect of such different frictional response, as a function of the temperature conditions, significantly affects the vibrational response of the tested material, as can be seen in Figure 13b. At 500 °C the dynamic response of the system, compared to the one observed at 300 °C (Figure 11), shows different features. At such a temperature condition, the instability is observed during the whole stroke, differently from 300°C test, in which it has been recorded only in the last part of the stroke. Moreover, at low velocities, when a negative slope is observable in the friction coefficient (Figure 13a), an increase in the amplitude of the vibrations is observed (Figure 13b), suggesting the overlapping of mode coupling and negative slope. At 500°C, the hypothesis of the coexistence of a negative slope and mode coupling instability is consistent with the outcomes obtained through the numerical model described in 2.3.3. In fact, it has been observed that the coexistence of mode coupling and negative slope leads to higher amplitude of the unstable friction-induced vibrations. Moreover, in the literature, the presence of a negative friction-velocity slope is often related to the occurrence of the stick-slip phenomenon [1, 3]. As shown in the spectrogram of Figure 13c, in the last part of braking, a broadband frequency excitation, due to stick-slip, is observed also in this case.

3.2.4 Experimental phase shift analysis

The method, based on the phase shift between normal and tangential accelerations, proposed in 2.4 to distinguish negative slope from mode coupling instability, has been validated experimentally. The phase shift analysis, performed on a single stroke taken at 500°C from a variable velocity test, is presented in Figure 14.

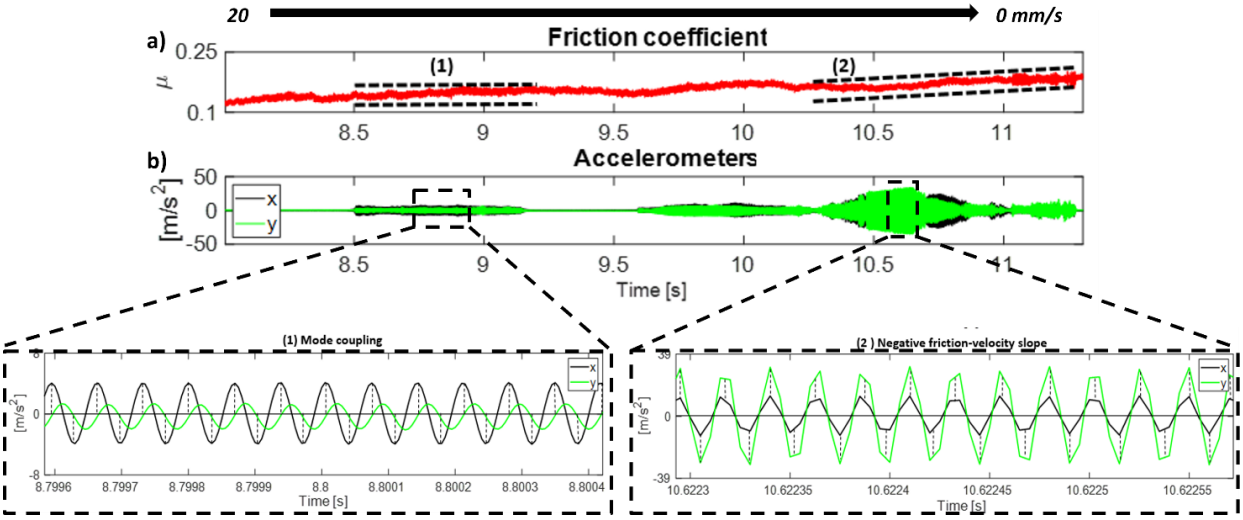

Figure 14 (adapted from [25]): 500°C single stroke: friction coefficient (a) and accelerometers (normal (y, green) and tangential (x, black)) signals (b). Obtained from HT 500°C variable velocity test. A focus on the phase shift between normal and tangential accelerations is provided for both mode coupling (1) and negative slope (2) instabilities

As can be seen from Figure 14, in correspondence of a constant friction coefficient (1), unstable vibrations, caused by mode coupling instability are recorded. The phase shift between normal (green) and tangential (black) accelerations has been analysed in correspondence of such unstable vibrations. A phase shift of almost 90° is observed. Conversely, in correspondence of a negative friction velocity slope relationship (2), unstable vibrations, due to negative slope instability, are recorded. Analysing the phase shift between normal and tangential accelerations, it can be seen that the two accelerations are almost in phase. The experimentally obtained results are consistent with the numerical one presented in 2.4, confirming the validity of the method proposed to distinguish negative slope from mode coupling instability.

4 Finite element model

A FEM model has been developed on ANSYS to reproduce and investigate the unstable modes observed experimentally. In the following sections, first, a description of the developed model is provided. Then, a prestressed modal analysis is presented.

4.1 Model description

Since the samples dynamic is the focus of the investigation, the reproduction of the whole test bench is not useful. For this reason, only the samples and sample holders of the entire test bench have been implemented in the model, as shown in Figure 15:

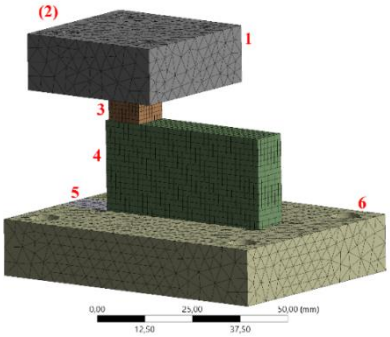

Figure 15: Model description: Upper sample-holder (1), upper block (not visible) (2), upper sample (3), lower sample (4), lower block (5), lower sample-holder (6)

As concerns the mesh, a compromise choice between the result accuracy and the computational time has been adopted. The mesh parameters are reported in Table 2:

Table 2: Mesh parameters

FEATURE	UPPER SAMPLE-HOLDER	UPPER SAMPLE	LOWER SAMPLE	LOWER SAMPLE-HOLDER
ELEMENT TYPE	Tet10	Hex20	Hex20	Tet10
ELEMENT SIZE [MM]	4	1,2	1,5	4
NO. ELEMENTS	4218	729	4046	10907

As concerns the contact regions, a frictional contact has been implemented only in the region between the two samples, with the Lagrange Multipliers method. For all other contacts (i.e., between samples and sample holders and between sample holders and blocks) a bonded contact is introduced by the penalty method. A 17 N load in vertical direction has been imposed through a static analysis. Moreover, a displacement of 1mm has been imposed to the lower part of the system to bring the contact in sliding condition for the prestressed modal analysis.

4.2 Prestressed modal analysis

The results of the prestressed modal analysis, performed under the conditions described in 4.1, are reported in Figure 16:

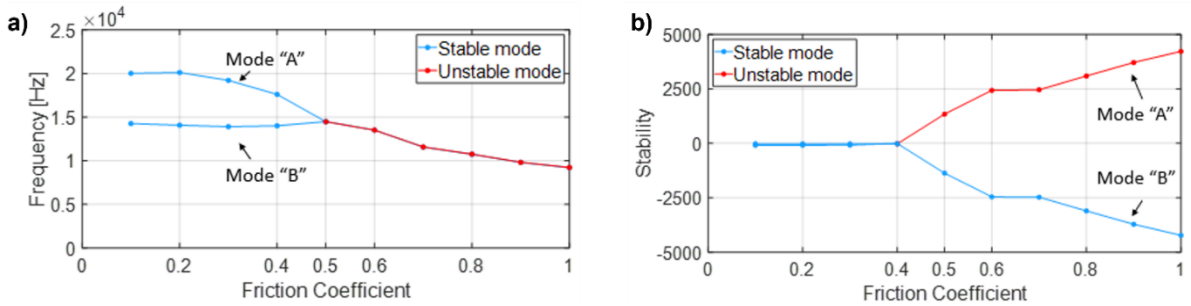

Figure 16: Frequency (a) and stability (b) of the analysed modes as a function of the friction coefficient.

As visible from Figure 16a, two modes of the system coalesce for a frequency of about 14.5kHz, as observed in the experimental campaign. The FEM model allows to visualize the mode shapes and deformations of the modes, reported in Figure 17.

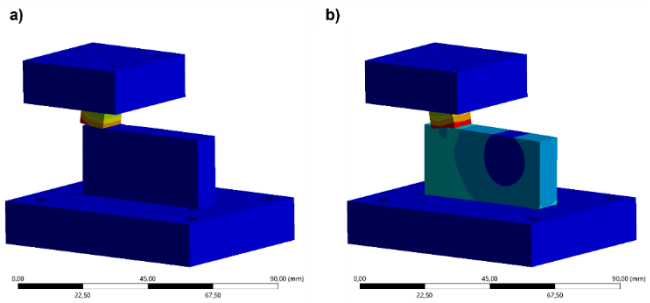

Figure 17: Mode "A" (a) and mode "B" (b): mode shapes (isometric view)

The involved modes show deformations mainly in tangential and normal directions with respect to the contact interface. Moreover, large deformations are retrieved for the upper sample.

5 Conclusions

This work investigated contact instabilities, either originated by mode-coupling or friction-velocity negative slope. The frictional and vibrational responses have been numerically and experimentally reproduced. As concerns the experimental measurement campaign, a characterization of a brake material has been carried out in order to investigate the material response under different temperatures and different sliding velocity conditions. A specifically designed test bench (TriboAir) has been used for such characterization under well-controlled boundary conditions. From the obtained data, the following main outcomes have been retrieved:

- A strong dependence of the material response on the working temperature has been observed;
- The occurrence of a negative friction-velocity slope, when the temperature is set to 300 °C, brings to the onset of contact instabilities due to such friction-velocity trend;
- For a temperature of 500 °C, the dynamic friction coefficient increases significantly, leading to mode coupling instability. Moreover, the presence of a negative slope during braking, at lower velocities, leads to strong unstable friction-induced vibrations due to the coexistence of mode coupling and negative friction-velocity slope instabilities.

As concerns the numerical part, two different models have been developed. A lumped-parameter model has been developed in order to investigate and characterize the onset of unstable friction-induced vibrations due to mode coupling and negative friction-velocity slope. The following results have been obtained:

- The system response under the coexistence of mode coupling and negative slope instabilities has been retrieved. It has been observed that the superposition of both phenomena leads to a higher amplitude of the unstable friction-induced vibrations. This outcome is consistent with the experimental results;
- The phase shift between the tangential and normal accelerations to the contact has been investigated, providing a method for identifying mode coupling and negative friction-velocity slope instability. It has been observed that, in presence of a negative friction-velocity slope instability, the vibrational signals are in phase. Conversely, a 90° degrees phase shift between the tangential and normal vibrational signals has been observed in presence of a mode coupling instability.

The FE numerical model allowed retrieving significant information to further characterize the dynamic response observed experimentally. A pre-stressed modal analysis has allowed investigating in more detail the occurrence of mode coupling. The system dynamics has been reproduced, obtaining a similar frequency of the unstable mode observed on the experimental system.

Acknowledgments

This research work was partially supported by EU project “AUDACITY”, Grant Agreement n. 831795.

A.L. acknowledges the French National Association of Research and Technology (ANRT) for its support to this work through the CIFRE convention N◦ 2018/1016.

References

[1] A. Akay, "Acoustics of friction," *The Journal of the Acoustical Society of America*, vol. 111, no. 4, pp. 1525-1548, 2002.

[2] N. M. Kinkaid, O. M. O'Reilly, and P. Papadopoulos, "Automotive disc brake squeal," *Journal of Sound and Vibration*, vol. 267, no. 1, pp. 105-166, 10/9/ 2003.

[3] H. Ouyang, W. Nack, Y. Yuan, and F. Chen, "Numerical analysis of automotive disc brake squeal: a review," *International Journal of Vehicle Noise and Vibration*, vol. 1, no. 3, pp. 207-231, 01/01/ 2005.

[4] A. Papangelo, N. Hoffmann, A. Grolet, M. Stender, and M. Ciavarella, "Multiple spatially localized dynamical states in friction-excited oscillator chains," *Journal of Sound and Vibration*, vol. 417, pp. 56-64, 2018/03/17/ 2018.

[5] D. Tonazzi et al., "Experimental and numerical characterization of system response under dry frictional contact," in *Proceedings of ISMA 2014 - International Conference on Noise and Vibration Engineering and USD 2014 - International Conference on Uncertainty in Structural Dynamics, 2014*, pp. 1931-1946.

[6] G. Ouenzerfi, F. Massi, E. Renault, and Y. Berthier, "Squeaking friction phenomena in ceramic hip endoprosthesis: Modeling and experimental validation," *Mechanical Systems and Signal Processing*, vol. 58, pp. 87-100, 2015.

[7] C. Weiss, P. Gdaniec, N. P. Hoffmann, A. Hothan, G. Huber, and M. M. Morlock, "Squeak in hip endoprosthesis systems: An experimental study and a numerical technique to analyze design variants," *Medical Engineering & Physics*, vol. 32, no. 6, pp. 604-609, 7// 2010.

[8] F. Massi, J. Rocchi, A. Culla, and Y. Berthier, "Coupling system dynamics and contact behaviour: Modelling bearings subjected to environmental induced vibrations and ‘false brinelling’ degradation," *Mechanical Systems and Signal Processing*, vol. 24, no. 4, pp. 1068-1080, 5// 2010.

[9] A. Guignabert et al., "Improvement of MSPA: Module of stepping piezo actuator," in *ACTUATOR 2018 - 16th International Conference and Exhibition on New Actuators and Drive Systems, Conference Proceedings*, 2018, pp. 121-124.

[10] D. W. Wang, J. L. Mo, M. Q. Liu, H. Ouyang, and Z. R. Zhou, "Noise performance improvements and tribological consequences of a pad-on-disc system through groove-textured disc surface," *Tribology International*, vol. 102, pp. 222-236, 2016.

[11] J. F. Brunel, P. Dufrénoy, and F. Demilly, "Modelling of squeal noise attenuation of ring damped wheels," *Applied Acoustics*, vol. 65, no. 5, pp. 457-471, 5// 2004.

[12] M. Di Bartolomeo, F. Morelli, D. Tonazzi, F. Massi, and Y. Berthier, "Investigation of the role of contact-induced vibrations in tactile discrimination of textures," *Mechanics & Industry*, 10.1051/meca/2017027 vol. 18, no. 4, // 2017.

[13] R. A. Ibrahim, "Friction-Induced Vibration, Chatter, Squeal, and Chaos—Part I: Mechanics of Contact and Friction," *Applied Mechanics Reviews*, vol. 47, no. 7, pp. 209-226, 1994.

[14] J.-J. Sinou and L. Jézéquel, "Mode coupling instability in friction-induced vibrations and its dependency on system parameters including damping," *European Journal of Mechanics - A/Solids*, vol. 26, no. 1, pp. 106-122, 1// 2007.

[15] D. Tonazzi, F. Massi, A. Culla, A. Fregolent, and Y. Berthier, "Role of damping on contact instability scenarios," in *5th World Tribology Congress, WTC 2013*, 2013, vol. 1, pp. 755-758.

[16] A. Papangelo, C. Putignano, and N. Hoffmann, "Critical thresholds for mode-coupling instability in viscoelastic sliding contacts," *Nonlinear Dynamics*, vol. 104, no. 4, pp. 2995-3011, 2021.

[17] K. Shin, M. J. Brennan, J. E. Oh, and C. J. Harris, "ANALYSIS OF DISC BRAKE NOISE USING A TWO-DEGREE-OF-FREEDOM MODEL," *Journal of Sound and Vibration*, vol. 254, no. 5, pp. 837-848, 2002/07/25/ 2002.

[18] D. Tonazzi, M. Passafiume, A. Papangelo, N. Hoffmann, and F. Massi, "Numerical and experimental analysis of the bi-stable state for frictional continuous system," *Nonlinear Dynamics*, vol. 102, no. 3, pp. 1361-1374, 2020.

[19] J. Brunetti, F. Massi, A. Saulot, and W. D'Ambrogio, "Modal dynamic instabilities generated by frictional contacts," in *5th World Tribology Congress, WTC 2013*, 2013, vol. 1, pp. 751-754.

[20] I. Ghezzi, D. Tonazzi, M. Rovere, C. Le Coeur, Y. Berthier, and F. Massi, "Tribological investigation of a greased contact subjected to contact dynamic instability," *Tribology International*, vol. 143, 2020, Art no. 106085.

[21] Z. Li, X. Wang, Q. Zhang, Z. Guan, J. Mo, and H. Ouyang, "Model reduction for friction-induced vibration of multi-degree-of-freedom systems and experimental validation," *International Journal of Mechanical Sciences*, vol. 145, pp. 106-119, 2018.

[22] A. Lazzari, D. Tonazzi, and F. Massi, "Squeal propensity characterization of brake lining materials through friction noise measurements," *Mechanical Systems and Signal Processing*, vol. 128, pp. 216-228, 2019/08/01/ 2019.

[23] F. Massi, L. Baillet, and A. Culla, "Structural modifications for squeal noise reduction: numerical and experimental validation," *International Journal of Vehicle Design*, vol. 51, no. 1, pp. 168-189, 01/01/ 2009.

[24] J. Brunetti, F. Massi, W. D'Ambrogio, and Y. Berthier, "Dynamic and energy analysis of frictional contact instabilities on a lumped system," (in English), *Meccanica*, pp. 1-15, 2014/08/07 2014.

[25] A. Lazzari, D. Tonazzi, J. Brunetti, A. Saulot, and F. Massi, "Contact instability identification by phase shift on C/C friction materials," *Mechanical Systems and Signal Processing*, vol. 171, 2022, Art no. 108902, doi: 10.1016/j.ymssp.2022.108902.